# Optimal Condition of DME Production through Syngas Hydrogenation in Dual Membrane Reactor

**Mohammad Farsi** * ⓘ , **Ahmad Hallajsani** ⓘ

1. Department of Chemical Engineering, School of Chemical and Petroleum Engineering,
2. Shiraz University, Shiraz, Iran. E-mail: farsi@shirazu.ac.ir
3. School of Chemical Engineering, College of Engineering, University of Tehran, Tehran, Iran. E-mail: hallaj@ut.ac.ir

| ARTICLE INFO | ABSTRACT |
|---|---|
| | Typically, supporting the dimethyl ether synthesis reactor by hydrogen and steam permselective membrane modules and optimization of operating conditions are practical solutions to shift the equilibrium conversion of reactions toward dimethyl ether synthesis and $CO_2$ conversion. In this regard, the aim of this research is to calculate the desired condition of hydrogen and steam Selective membrane reactors to improve dimethyl ether productivity. At first, the mass and energy conservation laws are applied to the membrane supported reactor to develop a heterogeneous model. After model validation, an optimization problem is programmed to calculate the optimal value of manipulated variables considering the limitations and constraints of the problem. Then, the main parameters of conventional and optimized membrane supported reactor including carbon monoxide and carbon dioxide conversion, dimethyl ether productivity, and temperature profiles are presented at steady-state conditions. The results of the simulation prove that dimethyl ether productivity is 0.0211 and 0.0262 mole $s^{-1}$ in conventional and optimized membrane reactors, respectively. In general, operating at optimal conditions increases DME production by up to 24.2%. |

## Introduction

Typically, DME as a colorless and organic compound is utilized as the synthetic fuel for compression ignition, refrigerant agent, aerosol spray propellant, and feed to produce dimethyl sulfate and acetic acid [1]. Currently, adopted environmental restrictions by governments and the need for alternative fuels have introduced DME as a synthetic fuel to mix with LPG and Diesel [2- 6]. Direct syngas conversion over a dual site catalyst and methanol dehydration over single site $Al_2O_3$ catalyst are two common routes of DME production. Due to the lower cost and higher equilibrium conversion, the direct DME production method is more attractive compared to the methanol dehydration method [7].

In this regard, much research have been conducted on DME production through the direct route and process planning to increase production capacity [8]. Vakili and Eslamloueyan designed a process to enhance the equilibrium conversion of syngas to DME [9]. The simulation results proved that the designed reaction system could enhance DME productivity by up to 12%. Lu et al. focused on the direct conversion of synthesis gas to DME in an non ideal reactor

* Corresponding Author: M. Farsi (E-mail address: farsi@shirazu.ac.ir)

[10]. The main benefits of applied fluidized bed against fixed bed reactor were lower pressure drop, higher carbon monoxide conversion, and higher DME productivity and yield. Papari et al. investigated the operability of slurry bubble column reactors to produce DME from syngas [11]. The considered reactor was modeled considering the two bubbles hydrodynamic flow approach. The results proved that the main benefit of a bubble column reactor is the uniform temperature in the system.

Although the combination of chemical reaction and separation makes the process more complex, it is a suitable technique to decrease operating costs and increase conversion. Iliuta et al. introduced the sorption-enhanced reaction process for syngas conversion to DME by in situ combination of chemical adsorption and reaction [12]. The simulation results showed that decreasing steam concentration in the reactor by chemical adsorption improves DME yield. The regeneration of saturated adsorbent was the critical section of the proposed process. Although supporting conventional reactors with the membrane module makes the process more complex and expensive, it shifts the equilibrium limited reactions toward the desired product. Since the hydrogenation of carbon monoxide and carbon dioxide and methanol dehydration are thermodynamically limited reactions, changing the concentration of components in the reaction zone, operating pressure and temperature could shift the reactions toward the DME production side. Mardanpour et al. simulated the syngas conversion to DME in a membrane supported reactor [13]. The results showed that increasing hydrogen concentration over the catalyst by applying a hydrogen permselective membrane module could enhance DME productivity. Falco et al. developed a Double Recycling Loop configuration to produce DME from carbon dioxide in a membrane supported reactor [14]. In the proposed structure, pure $CO_2$ was used as the sweep gas to shift $CO_2$ hydrogenation reaction toward the methanol synthesis. Farsi et al. designed a dual membrane supported configuration to enhance the equilibrium conversion of reactions in the direct DME synthesis route [15]. The results of the simulation proved that supporting the DME reactor by hydrogen and $H_2O$ permselective membrane modules was a useful approach to enhance rate of CO and $CO_2$ conversion and methanol dehydration reactions.

Although supporting the conventional reactor by membrane improved DME production, finding the optimal condition of a dual membrane supported reactor was a challenge and could enhance DME productivity [15]. In this regard, the aim of current research is to calculate the optimal operating condition of the considered membrane reactor to enhance the DME productivity. Thus, a constrained optimization problem is programmed and the optimal condition of the membrane supported reactor is determined considering the process limitations and bounds.

**Reaction Kinetics**

In general, the mixture of γ-$Al_2O_3$ and CuO–ZnO–$Al_2O_3$ catalysts are applied in the reactor to progress the rate of syngas conversion and methanol dehydration reactions, respectively [16]. The DME synthesis reaction network includes the hydrogenation of carbon monoxide, carbon dioxide, and methanol dehydration reactions. The hydrogenation of carbon monoxide and carbon dioxide to methanol reactions could be listed as:

$$2H_2 + CO + \leftrightarrow CH_3OH \qquad\qquad -\Delta H = 90.6 \text{ kJ mol}^{-1} \qquad\qquad (1)$$
$$3H_2 + CO_2 \leftrightarrow H_2O + CH_3OH \qquad\qquad -\Delta H = 49.4 \text{ kJ mol}^{-1} \qquad\qquad (2)$$

The methanol dehydration to DME reaction is as:

$$2CH_3OH \leftrightarrow H_2O + CH_3OCH_3 \qquad\qquad -\Delta H = 23.6 \text{ kJ mol}^{-1} \qquad\qquad (3)$$

The rate of carbon monoxide and carbon dioxide hydrogenation to methanol, and methanol dehydration reactions are as follows [17, 18]:

$$r_{CO} = \frac{k_1 f_{CO} f_{H_2}^2 (1 - \frac{f_{CH_3OH}}{K_{f1} f_{CO} f_{H_2}^2})}{(1 + K_{CO_2} f_{CO_2} + K_{CO} f_{CO} + K_{H_2} f_{H_2})^3} \tag{4}$$

$$r_{CO_2} = \frac{k_2 f_{CO_2} f_{H_2}^3 (1 - \frac{f_{CH_3OH} f_{H_2O}}{K_{f2} f_{CO_2} f_{H_2}^3})}{(1 + K_{CO_2} f_{CO_2} + K_{CO} f_{CO} + K_{H_2} f_{H_2})^4} \tag{5}$$

$$r_{DME} = \frac{k_3 f_{CH_3OH} (1 - \frac{f_{DME} f_{H_2O}}{K_{f3} f_{CH_3OH}^2})}{(1 + \sqrt{K_{CH_3OH} f_{CH_3OH}})^2} \tag{6}$$

## Process Modeling

### Reactor Modeling

Typically, the considered reactor includes three coaxial tubes that the annulus zone between the inner and middle tubes is packed by the solid catalyst. The inner tube is $H_2O$ permselective membrane and $H_2O$ permeates from the reaction zone toward the inner tube. The middle tube is hydrogen permselective and hydrogen is permeated from a hydrogen-rich stream to the reaction section. Since the carbon monoxide and carbon dioxide hydrogenation and methanol dehydration reactions are exothermic, the heat of reactions is removed by circulating saturated water around the outer tube. Table 1 presents the specifications of feed, and the characteristics of the reactor in the conventional DME synthesis process [19]. The diameter of the water permselective tube, reaction tube, and hydrogen permselective module are 38, 56.2, and 72 mm, respectively [15].

**Table 1**. Feed specification and characteristics of catalyst in the DME synthesis reactor

| | Parameter | Value | Unit |
|---|---|---|---|
| **Feed Specification** | Composition (mole fraction) | | |
| | Carbon monoxide | 17.16 | - |
| | Carbon dioxide | 4.09 | - |
| | Dimethyl ether | 0.18 | - |
| | Methanol | 0.3 | - |
| | Steam | 0.02 | - |
| | Hydrogen | 43.25 | - |
| | Nitrogen | 31.6 | - |
| | Methane | 4.4 | - |
| | Feed temperature | 493 | K |
| | Feed pressure | 50 | Bar |
| **Reactor Characteristics** | Pipe number | 4177 | - |
| | Pipe diameter | $\Phi 38 \times 2$ | mm |
| | Feed flow rate | $2.04 \times 10^5$ | $Nm^3 h^{-1}$ |
| | Reactor Length | 5.8 | M |
| | Shell temperature | 513 | K |
| | Wall heat conductivity | 48 | $Wm^{-1} K^{-1}$ |
| **Catalyst Data** | Diameter of catalyst | 5 | mm |
| | Bed density | 1200 | $Kg\ m^{-3}$ |
| | Bed porosity | 0.455 | - |

In this section, the considered model for membrane supported and conventional reactors are presented. The considered assumptions are:

- The ideal gas condition is valid.
- Since Pe is sufficiently large, radial dispersion of mass and energy is insignificant.
- Since Re is sufficiently large, the flow pattern in tubes is Plug.
- Since catalyst Bi is adequately small, the lumped body assumption is valid.

Based on the considered simplifications, the balance equations for the gas phase could be explained as:

$$u_g \frac{dC_i}{dz} + k_{gi}a_v(C_i - C_i^s) + \frac{\pi D_w}{A_R} Q_W - \frac{J_H}{A_R} = 0 \tag{7}$$

$$u_g\rho_g C_{pg} \frac{dT}{dz} + h_f a_v(T - T^s) + \frac{\pi D_w}{A_R} U_{rw}(T - T_w) + \frac{\pi D_r}{A_h} U_{rh}(T - T_H) = 0 \tag{8}$$

The governing equations for solid phases could be explained as:

$$\eta_i \rho_B r = k_{gi}a_v(C_i - C_i^s) \tag{9}$$

$$\eta_i \rho_B r(-\Delta H) = h_f a_v(T - T^s) \tag{10}$$

The governing equations for water permselective module are:

$$u_m \frac{dC_w}{dz} - \frac{\pi D_m}{A_m} Q_w = 0 \tag{11}$$

$$u_m\rho_m C_{pm} \frac{dT}{dz} - \frac{\pi D_w}{A_R} U_{rw}(T - T_w) = 0 \tag{12}$$

The governing equations for the hydrogen permselective module are:

$$u_m \frac{dC_H}{dz} + \frac{J_H}{A_m} = 0 \tag{13}$$

$$u_h\rho_h C_{ph} \frac{dT}{dz} - \frac{\pi D_r}{A_h} U_{rh}(T - T_H) + \frac{\pi D_h}{A_h} U(T_H - T_{sh}) = 0 \tag{14}$$

Table 2 presents the applied correlation to calculate the thermal and physical properties of components and transfer resistances.

**Table 2**. The characteristics of hydrogen and water membrane modules

| Parameter | Correlation | Ref. |
|---|---|---|
| Specific heat capacity | $c_p = a + bT + cT^2 + dT^3$ | |
| Viscosity | $\mu = \dfrac{c_1 T^{c_2}}{1 + \dfrac{c_3}{T} + \dfrac{c_4}{T^2}}$ | (22) |
| Diffusion mass transfer coefficient | $D_{im} = \dfrac{1 - y_i}{\displaystyle\sum_{i=j} \dfrac{y_i}{D_{ij}}}$ | (23) |
| Mass transfer coefficient | $k_{gi} = 1.17 Re^{-0.42} Sc_i^{-0.67} u_g 10^3$ | (24) |
| Overall heat transfer coefficient | $\dfrac{1}{U} = \dfrac{1}{h_i} + \dfrac{A_i \ln \left(\frac{D_o}{D_i}\right)}{2\pi L K_w} + \dfrac{A_i}{A_o} \dfrac{1}{h_o}$ | |
| Convective heat transfer coefficient | $\dfrac{h}{c_p \rho \mu} \left(\dfrac{c_p \mu}{K}\right)^{2/3} = \dfrac{0.458}{\varepsilon_B} \left(\dfrac{\rho u d_p}{\mu}\right)^{-0.407}$ | (25) |

## Water Membrane Tube

Since $H_2O$ is produced through $CO_2$ hydrogenation and methanol dehydration reactions, decreasing the concentration of $H_2O$ in the reaction zone by the applied membrane module could increase equilibrium conversion of both reactions. The $H_2O$ permeation rate through the applied alumina-silica composite membrane could be calculated by [20]:

$$Q_i = \pi_w (P_w^R - P_w^S) \tag{15}$$

## Hydrogen Membrane

In general, increasing the concentration of hydrogen could progress the carbon monoxide and carbon dioxide hydrogenation reactions toward the methanol synthesis side and consequently enhances the rate of MeOH dehydration. The rate of hydrogen permeation through Pd-Ag membrane module could be calculated as:

$$J_h = 6.33 \times 10^{-8} \frac{2\pi\, e^{-\frac{E_p}{RT}}}{ln\,(R_o/R_i)} \left(\sqrt{P_h^R} - \sqrt{P_h^S}\right) \tag{16}$$

## Process Optimization

Optimization is a practical approach to determine the desired inputs of a system considering limitations and constraints. The main steps in process optimization are process modeling, defining the objective function, and selection of available inputs and bounds. Typically, the goal in DME synthesis plans is to enhance the production capacity without violating constraints and bounds. In this regard, DME productivity has been chosen as the objective function. In addition, inlet syngas pressure, inlet syngas temperature, feed temperature of inlet sweep gas to hydrogen and $H_2O$ permselective sides, and temperature of circulating water have been selected as the decision variables. Thermodynamically, changing operating pressure and temperature change equilibrium constant of reactions and could increase equilibrium conversion of reactions. In addition, increasing temperature causes catalyst deactivation by sintering and coke formation. Although increasing operating pressure shifts the hydrogenation of carbon monoxide and carbon dioxide reactions toward the methanol synthesis side, there is a maximum operating condition based on the reactor design pressure. Besides, the operating pressure affects the rate of hydrogen and $H_2O$ permeation along the applied membrane modules. In this regard, 533K

and 70 bar have been selected as the upper bound of temperature and pressure, respectively. The genetic algorithm method, with 200 generations and 150 populations, is used to calculate the optimal condition of a dual membrane supported reactor [21].

**Numerical Solution**

The obtained equations in the modeling section provide a set of mixed non-linear differential and algebraic equations. These equations are solved numerically by the Forth Order Runge Kutta method.

# Results and Discussions

**Model Validation**

Since the established mathematical model is utilized in the optimization stage, the precision of optimization results depends on the accuracy of the reactor model. The comparison of the model results and available data points is tabulated in Table 4 at the same feed condition. As seen in Table 3, there is a tolerable error between data points and the results of the simulation, and the model results is valid.

**Table 3**. Utilized equations to estimate the transfer coefficient, physical and thermal properties

|  | Hu et al. | Result of Model | Relative Error (%) |
|---|---|---|---|
| DME | 0.0491 | 0.0509 | 3.66 |
| CO | 0.0877 | 0.0851 | -2.9 |
| $CO_2$ | 0.0671 | 0.0674 | 0.44 |
| Outlet temperature (K) | 516.7 | 519.8 | 0.59 |

**Process Optimization**

Although the dual membrane configuration is more efficient over the conventional DME reactor, applying the optimal value of manipulated variables on the membrane supported reactor enhances DME productivity considerably. the calculated optimum condition of dual membrane supported reactor is shown in Table 4. Typically, DME productivity in the conventional and optimized membrane supported reactors are 0.0262 and 0.0211 mole s$^{-1}$, respectively. Applying optimal value of manipulated variables on the system enhances DME productivity up to 24.17%.

**Table 4**. Comparing simulation results and taken data points from industrial plant

| Decision variables | Value |
|---|---|
| Feed Temperature (K) | 515.4 |
| Inlet sweep gas in water side (K) | 508.6 |
| Inlet sweep gas in hydrogen side (K) | 494.7 |
| Circulating water side (K) | 503.3 |
| Feed pressure (Bar) | 60.6 |
| DME production rate | 0.0262 |

Increasing operating pressure shifts the methanol synthesis reactions in the direction of CO and $CO_2$ hydrogenation and enhances the syngas equilibrium conversion. Then, the produced methanol through hydrogenation reactions is dehydrated and converted to DME. On the other hand, increasing the pressure of the reaction zone could reduce the partial pressure difference between the sweep gas and reaction zone and result in lower hydrogen permeation. Thus, there

is an optimum operating pressure to set DME productivity at the highest value. The difference between the calculated optimal pressure and the considered upper bound for pressure proves that the applied pressure constraint is inactive. Thus, the process is safe and fluctuation of feed pressure during the process run time does not make the process risky. Fig. 1 illustrates the DME productivity profile along the conventional and optimized membrane supported reactors. It appears that hydrogen permeation from the hydrogen-rich stream toward the reaction increases the concentration of hydrogen over the catalyst and shifts methanol synthesis reactions toward methanol productivity. In addition, decreasing the concentration of $H_2O$ over the catalyst shifts carbon monoxide and carbon dioxide hydrogenation and DME synthesis reactions toward the completion. Thus, applied membrane modules to increase the concentration of hydrogen and decrease the concentration of $H_2O$ over the catalyst and operating at optimized condition have a positive impact on the reaction network and improves the DME yield.
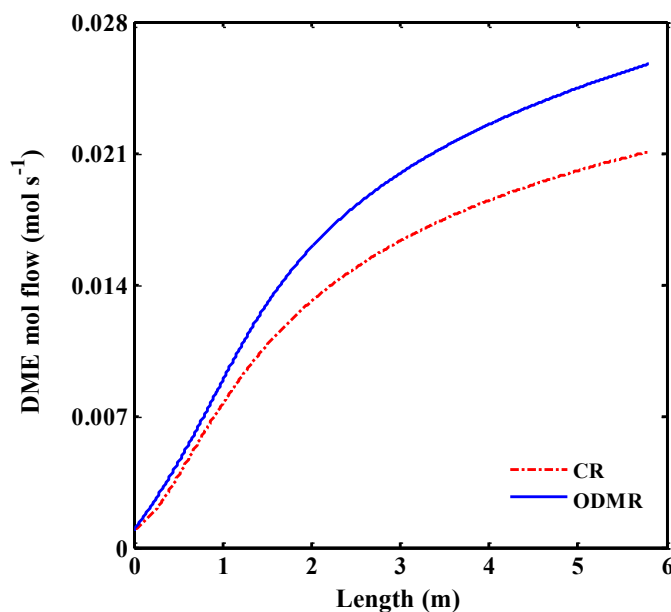


**Fig. 1**. Flow rate of DME in the conventional and optimized membrane supported reactors

Fig. 2 explains the profile of gas temperature along the conventional and optimized membrane supported reactors. Although increasing operating temperature enhances the rate of methanol synthesis and dehydrogenation reaction, it has a negative impact on the final conversion of exothermic reactions and reduces the equilibrium conversion in those reactions. Theoretically, increasing the reaction rate by applying hot feed and overcoming the equilibrium limitations by reducing the temperature at the second part is the optimal temperature trajectory along the reactor. In this regard, the developed optimal temperature trajectory along the dual membrane reactor enhances the DME productivity. As seen the heat production by the reaction is dominant over the energy transfer at the first half of the reaction zone and temperature increases gradually. Since the concentration of reactants decreases along the reactor, the rate of energy transfer is dominant over the energy production rate in the second part and temperature decreases gradually. Since the hydrogen permselective zone creates an extra heat transfer resistance to remove the heat of the reaction, a higher temperature is developed in the membrane supported reactor against the conventional reactor.
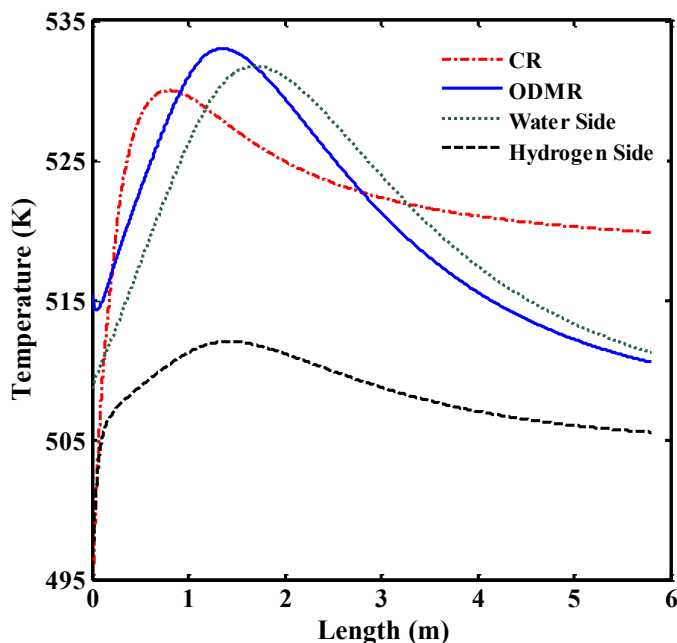
**Fig. 2**. Profile of temperature in the conventional and optimized dual membrane supported reactors

Fig. 3 presents the carbon monoxide profile in the conventional and optimized membrane supported reactors. In addition, Figs. 4a and b illustrate the carbon dioxide content and rate of carbon dioxide hydrogenation along the conventional and optimized membrane supported reactors. Typically, the applied changes in the system shift the carbon monoxide hydrogenation reaction in the direction of the completion reaction and improve the rate methanol dehydration to DME by increasing methanol concentration in the system. Besides, since equilibrium constant of the $CO_2$ hydrogenation reaction is small, increasing methanol concentration in the system via progress of CO hydrogenation reaction shifts the hydrogenation of carbon dioxide reaction in the reverse direction. The results of simulation illustrate that the $CO_2$ productivity are 0.0279 and 0.0247 mole $s^{-1}$ in the conventional and optimized reactors, respectively.
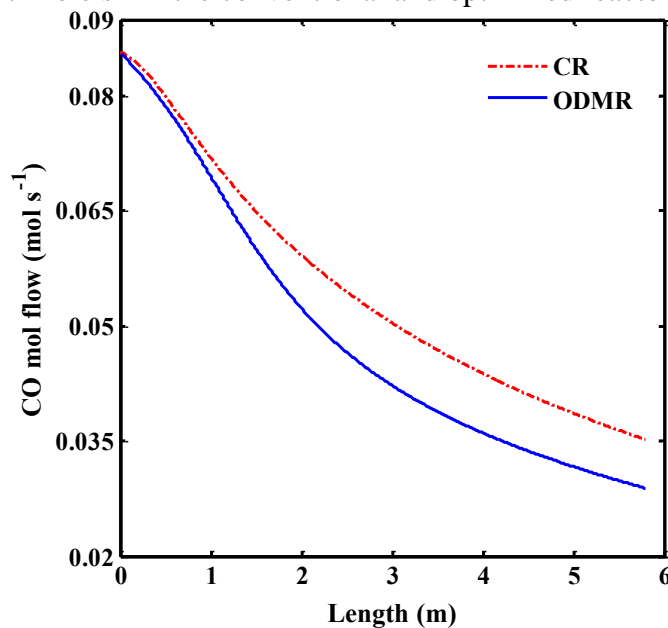


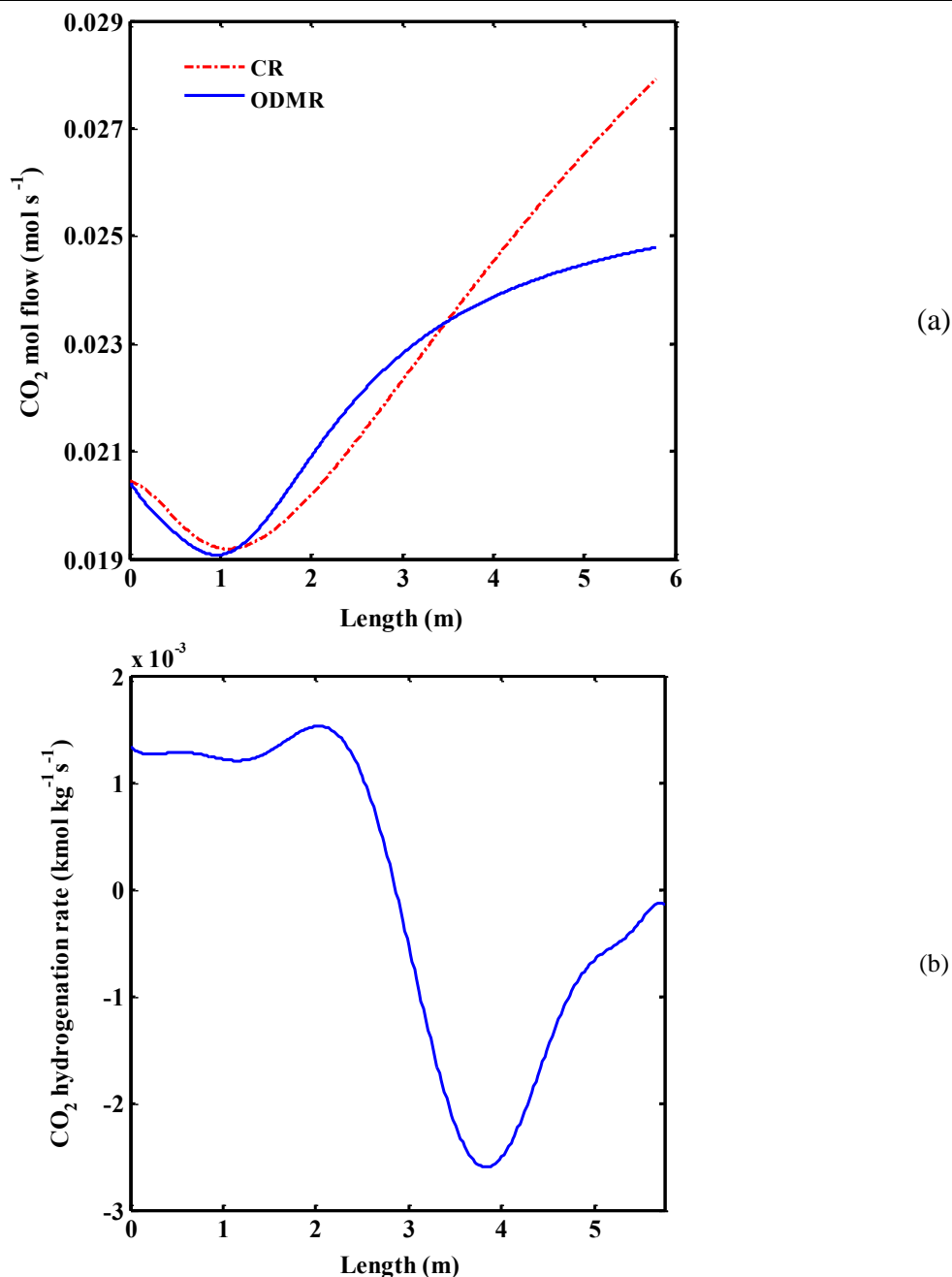**Fig. 3**. Flow rate of CO in the conventional and optimized membrane supported reactors

**Fig. 4**. (a) flow rate of $CO_2$ and (b) rate of $CO_2$ hydrogenation along the conventional and optimized dual membrane supported reactors

The hydrogen and $H_2O$ content along the conventional and membrane supported reactors have been presented in Figs. 5 and 6, respectively. Although methanol synthesis reactions decrease hydrogen concentration in the conventional reactor, hydrogen-rich sweep gas act as a hydrogen source for CO and $CO_2$ hydrogenation reactions, and a part of the consumed hydrogen is supplied by an applied membrane module. The results of the simulation show that the permeation rate of hydrogen dominates over the hydrogen consumption rate and hydrogen concentration increases at the last part of the dual membrane supported reactor. Besides, the steam productivity through $CO_2$ hydrogenation and methanol dehydration reactions is dominants over the rate of steam permeation and $H_2O$ concentration increases along the optimized membrane supported reactor continuously.
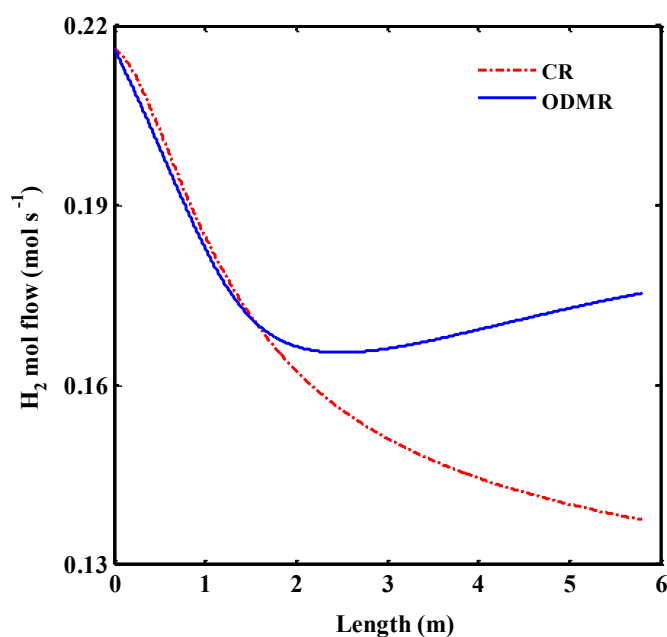
**Fig. 5**. Flow rate of $H_2$ in the conventional and optimized membrane supported reactors
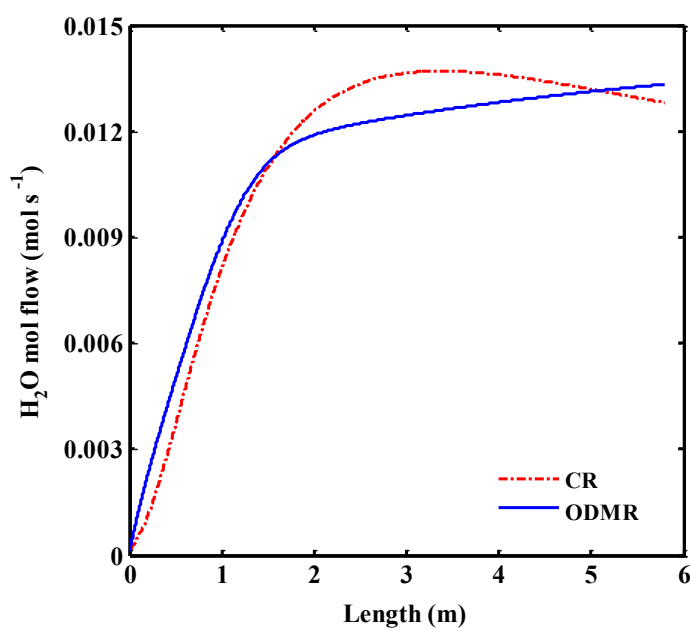


**Fig. 6**. Flow rate of $H_2O$ in the conventional and optimized membrane supported reactors

## Conclusions

In this research, the optimal value of manipulated variables in the hydrogen and steam perm-selective membrane reactor was determined to set DME productivity at the maximum value. The considered isothermal reactor was mathematically modeled considering internal and external mass and heat diffusion limitations. To optimize the process performance, an optimization problem was programmed considering DME productivity as the objective function, feed pressure, feed temperature, the inlet temperature of sweep gas flow rate and boiling water temperature as decision variables. The Genetic Algorithm method was applied to

handle the programmed optimization problem. The results of the simulation proved that DME production was enhanced up to 24.17% in the optimized membrane supported reactor compared to the conventional process. Besides, carbon dioxide emission was decreased by about 11.5% in the optimal dual membrane reactor. In general, the applied membrane modules enhanced DME productivity, carbon dioxide and carbon monoxide conversion, and enhanced catalyst lifetime by changing the concentration of hydrogen and steam over the applied catalyst.

## Nomenclature

| | |
|---|---|
| $A_c$ | Cross section area (m$^2$) |
| $a_v$ | Catalyst specific surface area (m$^2$ m$^{-3}$) |
| $C_i$ | Concentration (mol m$^{-3}$) |
| $C_p$ | Specific heat capacity (J mol$^{-1}$ K$^{-1}$) |
| $D$ | Diameter (m) |
| $F$ | Molar flow rate (mol s$^{-1}$) |
| $f_i$ | Fugacity of component i, (bar) |
| $\Delta H$ | Heat of reaction (J mol$^{-1}$) |
| $h_f$ | Heat transfer coefficient (W m$^{-2}$ K$^{-1}$) |
| $k$ | Arrhenius factor of reaction rate (mol kg$^{-1}$ s$^{-1}$ bar$^{-1/2}$) |
| $k_g$ | Mass transfer coefficient (m s$^{-1}$) |
| $L$ | Length (m) |
| $P$ | Pressure (bar) |
| $ri$ | rate of reaction (mol kg$^{-1}$ s$^{-1}$) |
| $R$ | Universal gas constant [Pa m$^3$ mol$^{-1}$ K$^{-1}$] |
| $T$ | Temperature (K) |
| $u$ | Superficial velocity (m s$^{-1}$) |
| $U$ | Overall heat transfer coefficient (W m$^{-2}$ K$^{-1}$) |
| $z$ | Axial coordinate (m) |

Greek Letters

| | |
|---|---|
| $\alpha_h$ | Hydrogen flux constant (mol s$^{-1}$ m$^{-1}$ Pa$^{-1/2}$) |
| $\mu$ | Viscosity (kg m$^{-1}$ s$^{-1}$) |
| $\rho$ | Density (kg m$^{-3}$) |
| $\pi_w$ | Steam flux constant, (mol m$^{-2}$ s$^{-1}$Pa$^{-1}$) |
| $\varepsilon$ | Bed void fraction |

Superscripts and Subscripts

| | |
|---|---|
| g | Gas phase |
| H | Hydrogen membrane side |
| m | Water Membrane side |
| r | Reaction side |
| s | Catalyst surface |
| t | Tube side |
| W | Water vapor membrane side |

## References

[1]  Ng KL, Chadwick D, Toseland B. Kinetics and modelling of dimethyl ether synthesis from synthesis gas. Chemical Engineering Science. 1999;54(15):3587-92. https://doi.org/10.1016/S0009-2509(98)00514-4

[2]  Alam M, Fujita O, Ito K. Performance of NOx reduction catalysts with simulated dimethyl ether diesel engine exhaust gas. Proceedings of the Institution of Mechanical Engineers, Part A: Journal of Power and Energy. 2004;218(2):89-95.

[3]     Fleisch T, Basu A, Gradassi M, Masin J. Dimethyl ether: a fuel for the 21st century. studies in surface science and catalysis. 1997; 107:117-25. https://doi.org/10.1016/S0167-2991(97)80323-0

[4]     Rouhi A. Amoco, Haldor-Topsoe Develop Dimethyl Ether as Alternative Diesel Fuel. Chemical & Engineering News. 1995;73(22):37-9.

[5]     Song J, Huang Z, Qiao X, Wang W. Performance of a controllable premixed combustion engine fueled with dimethyl ether. Energy Conversion and Management. 2004;45(13):2223-32. https://doi.org/10.1016/j.enconman.2003.11.004

[6]     Sorenson SC. Dimethyl ether in diesel engines: progress and perspectives. Journal of Engineering for Gas Turbines and Power. 2001;123(3):652-8. https://doi.org/10.1115/1.1370373

[7]     Brown DM, Bhatt BL, Hsiung TH, Lewnard JJ, Waller FJ. Novel technology for the synthesis of dimethyl ether from syngas. Catalysis Today. 1991;8(3):279-304. https://doi.org/10.1016/0920-5861(91)80055-E

[8]     Nie Z, Liu H, Liu D, Ying W, Fang D. Intrinsic kinetics of dimethyl ether synthesis from syngas. J Nat Gas Chem. 2005;14(1):22-8.

[9]     Vakili R, Eslamloueyan R. Optimal design of an industrial scale dual-type reactor for direct dimethyl ether (DME) production from syngas. Chemical Engineering and Processing: Process Intensification. 2012; 62:78-88. https://doi.org/10.1016/j.cep.2012.09.00

[10]    Lu W-Z, Teng L-H, Xiao W-D. Simulation and experiment study of dimethyl ether synthesis from syngas in a fluidized-bed reactor. Chemical Engineering Science. 2004;59(22):5455-64. https://doi.org/10.1016/j.ces.2004.07.03

[11]    Papari S, Kazemeini M, Fattahi M. Mathematical modeling of a slurry reactor for DME direct synthesis from syngas. Journal of Natural Gas Chemistry. 2012;21(2):148-57. https://doi.org/10.1016/S1003-9953(11)60347-2

[12]    Iliuta I, Iliuta MC, Larachi F. Sorption-enhanced dimethyl ether synthesis—Multiscale reactor modeling. Chemical Engineering Science. 2011;66(10):2241-51. https://doi.org/10.1016/j.ces.2011.02.047

[13]    Mardanpour MM, Sadeghi R, Ehsani MR, Esfahany MN. Enhancement of dimethyl ether production with application of hydrogen-permselective Pd-based membrane in fluidized bed reactor. Journal of Industrial and Engineering Chemistry. 2012;18(3):1157-65. https://doi.org/10.1016/j.jiec.2012.01.012

[14]    De Falco M, Capocelli M, Giannattasio A. Membrane Reactor for one-step DME synthesis process: Industrial plant simulation and optimization. Journal of CO2 Utilization. 2017; 22:33-43. https://doi.org/10.1016/j.jcou.2017.09.008

[15]    Farsi M, Sani AH, Riasatian P. Modeling and operability of DME production from syngas in a dual membrane reactor. Chemical Engineering Research and Design. 2016; 112:190-8. https://doi.org/10.1016/j.cherd.2016.06.019

[16]    Nie Z-g, Fang D-y. Global Kinetics of Direct Synthesis of Dimethyl Ether from Syngas Containing N~ 2 over Bifunctional Mixed Catalyst. Journal-East China University of Science and Technology. 2004;30(4):370-4.

[17]    Song W, Zhu B, Wang H, Zhu M, Sun Q, Zhang J. Reaction kinetics of methanol synthesis in the presence of C301 Cu-based catalyst (I) model of intrinsic kinetics. J. Chem. Ind. Eng. 1988; 39:401-8.

[18]    Zhang H-t, Cao F-h, Liu D-h. Thermodynamic analysis for synthesis of dimethyl ether and methanol from synthesis gas. Journal-East China University of Science and Technology. 2001;27(2):198-201.

[19]    Hu Y, Nie Z, Fang D. Simulation and model design of pipe-shell reactor for the direct synthesis of dimethyl ether from syngas. Journal of Natural Gas Chemistry. 2008;17(2):195-200. https://doi.org/10.1016/S1003-9953(08)60051-1

[20]    Lee K-H, Youn M-Y, Sea B. Preparation of hydrophilic ceramic membranes for a dehydration membrane reactor. Desalination. 2006;191(1):296-302. https://doi.org/10.1016/j.desal.2005.07.026

[21]    Haupt RL, Haupt SE. Practical genetic algorithms: John Wiley & Sons; 2004.
[22]    Perry R, Green D, Maloney J. Perry's chemical Engineers' handbook: McGraw-Hill; 1997.
[23]    Wilke C. Estimation of liquid diffusion coefficients: Chemical Engineering Progress; 1949.
[24]    Cussler EL. Diffusion: mass transfer in fluid systems: Cambridge university press; 2009.
[25]    Smith JM. Chemical Engineering Kinetics. McGraw-Hill; 1981.